Separator Effects on Lithium Plating and Stripping Reversibility and Performance of High-Voltage Lithium metal batteries

Boyu Zhu

A thesis

submitted in partial fulfillment of the

requirements for the degree of

Master of Science

University of Washington

2026

Committee:

Jun Liu

Mitchell Kaiser

Program Authorized to Offer Degree:

Materials Science and Engineering

University of Washington

Abstract

Separator Effects on Lithium Plating and Stripping Reversibility and Performance of High-Voltage Lithium metal batteries

Boyu Zhu

Chair of the Supervisory Committee:

Jun Liu

Department of Materials Science and Engineering

Polyolefin separators play a central role in regulating ion transport and interfacial stability in lithium metal batteries, yet their performance can vary markedly across testing environments. In this study, Celgard 2400 and Celgard 2500 polypropylene separators, the Celgard 2325 trilayer separator, and a Nanoshel polyethylene separator were systematically compared in CR2032 cells under controlled assembly conditions with fixed electrolyte volume and consistent cell hardware through both Li|Cu plating/stripping tests and high-voltage NMC811|Li full-cell cycling. In Li|Cu cells, all separators exhibited high coulombic efficiency, but a reproducible separator dependence emerged, with cells using Celgard 2400 and Celgard 2500 polypropylene separators showing higher efficiency than those using the polyethylene separator and Celgard 2400 delivering the highest average value. Replicate statistics further indicated small yet measurable scatter, highlighting that instrument precision can contribute to apparent fluctuations when efficiencies approach unity. In contrast, separator ranking changed in full cells cycled between 2.8 and 4.4 V, where the polyethylene separator provided the highest capacity retention, coulombic efficiency closest to unity, and the most stable long-term cycling behavior, while Celgard 2325 trilayer separator exhibited the poorest durability with pronounced late-cycle instability. These findings indicate that separator performance is not universal but depends strongly on the battery chemistry and operating conditions.

Separator Effects on Lithium Plating and Stripping Reversibility and Performance of High-Voltage Lithium metal batteries

By: Boyu Zhu

Materials Science and Engineering

University of Washington

Supervisor: Jun Liu

Abstract

Polyolefin separators play a central role in regulating ion transport and interfacial stability in lithium metal batteries, yet their performance can vary markedly across testing environments. In this study, Celgard 2400 and Celgard 2500 polypropylene separators, the Celgard 2325 trilayer separator, and a Nanoshel polyethylene separator were systematically compared in CR2032 cells under controlled assembly conditions with fixed electrolyte volume and consistent cell hardware through both Li|Cu plating/stripping tests and high-voltage NMC811|Li full-cell cycling. In Li|Cu cells, all separators exhibited high coulombic efficiency, but a reproducible separator dependence emerged, with cells using Celgard 2400 and Celgard 2500 polypropylene separators showing higher efficiency than those using the polyethylene separator and Celgard 2400 delivering the highest average value. Replicate statistics further indicated small yet measurable scatter, highlighting that instrument precision can contribute to apparent fluctuations when efficiencies approach unity. In contrast, separator ranking changed in full cells cycled between 2.8 and 4.4 V, where the polyethylene separator provided the highest capacity retention, coulombic efficiency closest to unity, and the most stable long-term cycling behavior, while Celgard 2325 trilayer separator exhibited the poorest durability with pronounced late-cycle instability. These findings indicate that separator performance is not universal but depends strongly on the battery chemistry and operating conditions.

1.Introduction, background and motivation

1.1 Introduction

Lithium metal is widely viewed as a cornerstone anode for next-generation rechargeable batteries because its exceptionally high theoretical specific capacity and very low electrochemical potential offer a clear pathway toward higher energy density than conventional graphite-based systems. [1] In principle, pairing lithium metal with high-capacity cathodes can substantially increase cell-level energy density while also enabling battery chemistries that are difficult to realize with graphite. At the same time, lithium metal is attractive from a manufacturing and materials standpoint because it can serve as an anode-free or limited-lithium configuration, where the negative electrode inventory is minimized and energy density is further improved.

However, in practical cells, lithium-metal cycling is often limited by poor plating and stripping reversibility and by persistent interfacial instability. During repeated deposition and dissolution, the Li–electrolyte interface can undergo continuous side reactions and experience non-uniform reaction and transport conditions. These processes consume active lithium and electrolyte, form heterogeneous interphase layers, increase polarization, and gradually degrade cycling performance. In addition, non-uniform depositions can generate rough, porous, or filamentary lithium morphologies, which not only accelerate interfacial area growth and parasitic reactions but can also create severe local current-density amplification during subsequent cycling. In such morphologies, portions of deposited lithium may become electronically isolated and transform into electrochemically inactive “dead Li,” further lowering the apparent reversibility and amplifying heterogeneity. The coupled nature of transport, interfacial chemistry, and morphology evolution makes lithium-metal failure modes strongly dependent on both materials choices and operating conditions.

While electrolyte engineering and interphase design have delivered substantial progress, the separator remains an equally important component that can strongly influence lithium deposition behavior but is sometimes treated as a fixed background choice. The separator is not only a passive

electronic insulator. As a porous transport medium, it defines the effective ionic pathways between electrodes and therefore shapes concentration gradients, local electrolyte depletion, and the distribution of overpotential under applied current. [2] Under practical current densities, even modest differences in transport resistance and pore-network architecture can translate into different degrees of salt depletion near the lithium surface, which can shift the deposition regime from relatively stable growth to localized, morphology-amplifying growth.

In this sense, separator properties such as thickness, porosity, tortuosity and pore connectivity, pore size distribution, and electrolyte wetting can modulate the uniformity of Li^+ flux reaching the lithium surface. This in turn influences whether lithium deposits more homogeneously or concentrates into local hotspots that promote surface roughening and increase the risk of penetration. Separators also interact with the electrolyte in ways that go beyond simple wettability. Polymer chemistry and surface treatments can affect electrolyte uptake, interfacial impedance, and the stability of the separator structure during cycling, while mechanical properties can influence how the separator tolerates pressure, deformation, and potential contact with protruding lithium features. Because commercial separators made from polyethylene, polypropylene, and polypropylene–polyethylene multilayer architectures differ simultaneously in polymer chemistry and microstructural transport characteristics, it is not obvious that any single separator family is universally optimal across different electrolytes and cycling protocols. Instead, separator selection is better viewed as a coupled design problem that depends on the electrolyte formulation, the areal capacity and current density, the cell format and stack pressure, and the intended cycling window.

This study aims to investigate whether and how commercial separator properties influence lithium-metal plating/stripping behavior and full-cell performance, providing experimental insights into the interplay between separator pore-network transport, electrolyte–separator interfacial chemistry, and the evolution of lithium deposition morphology. By systematically comparing representative polyethylene (PE), polypropylene (PP), and PP–PE multilayer separators under controlled Li|Cu half-cell and Li||NMC full-cell protocols, this work seeks to clarify how transport resistance, pore

connectivity, and wettability govern lithium reversibility in half cells and, when coupled with high-voltage parasitic reactions and cathode-derived species in full cells, manifest as polarization growth, lithium inventory loss, and failure modes such as short circuits. The findings could pave the way for separator-centered selection guidelines tailored to battery chemistry and operating conditions, contributing to the broader field of high-energy rechargeable lithium-based batteries.

1.2. Background and Motivation

Lithium metal batteries promise high energy density, yet practical operation is often limited by non-uniform lithium deposition and continuous interfacial side reactions. During charging, lithium ions travel through the separator and deposit on the negative side. Any spatial non uniformity in ion transport can amplify local current density at surface protrusions, accelerating rough growth, increasing interfacial area, and promoting the formation of electrochemically inactive lithium. These coupled transport and interfacial processes can ultimately lead to rapid polarization growth and, in severe cases, internal short circuits.

Figure 1 illustrates a mechanistic picture of how the separator can influence lithium deposition. In a baseline configuration, heterogeneous ion flux can concentrate near surface asperities, leading to locally accelerated plating and the development of thick, non-uniform interphase and lithium morphologies. In contrast, an engineered separator or interlayer concept can redistribute lithium-ion transport and regulate interfacial chemistry near the lithium surface, resulting in more spatially uniform deposition and a more stable interphase. This schematic highlights a central motivation for separator focused studies, namely that the separator is not merely a physical barrier but a transport medium whose pore network and surface chemistry can alter the local electrochemical environment at the lithium interface.

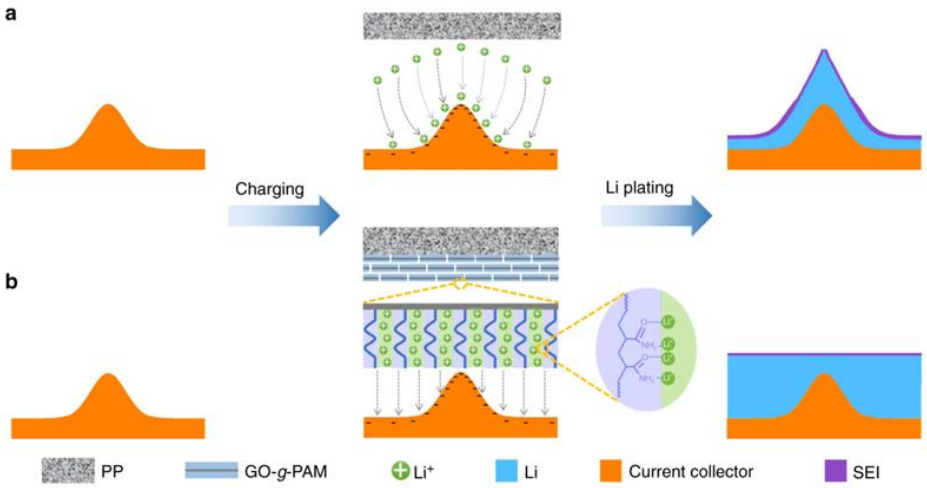

Figure. 1. Schematic diagram of Li deposition on electrodes with microscopic surface roughness [3]

Because separator effects arise from multiple coupled attributes, it is useful to frame separator selection through a set of key properties rather than a single descriptor. Figure 2 summarizes the major property classes that govern separator function, including structure related parameters such as thickness, porosity, and pore structure, intrinsic materials related parameters such as ionic conductivity, wettability, electrochemical stability, and chemical stability, and robustness related parameters such as thermal dimensional stability, puncture strength, tensile strength, shutdown temperature, and melt integrity. In lithium metal cells, transport related properties strongly affect concentration gradients and local overpotential under load, while chemical and electrochemical stability become increasingly important in high voltage full cell operation where oxidative electrolyte decomposition, cathode derived species, and pore blocking by decomposition products can raise resistance and accelerate degradation.

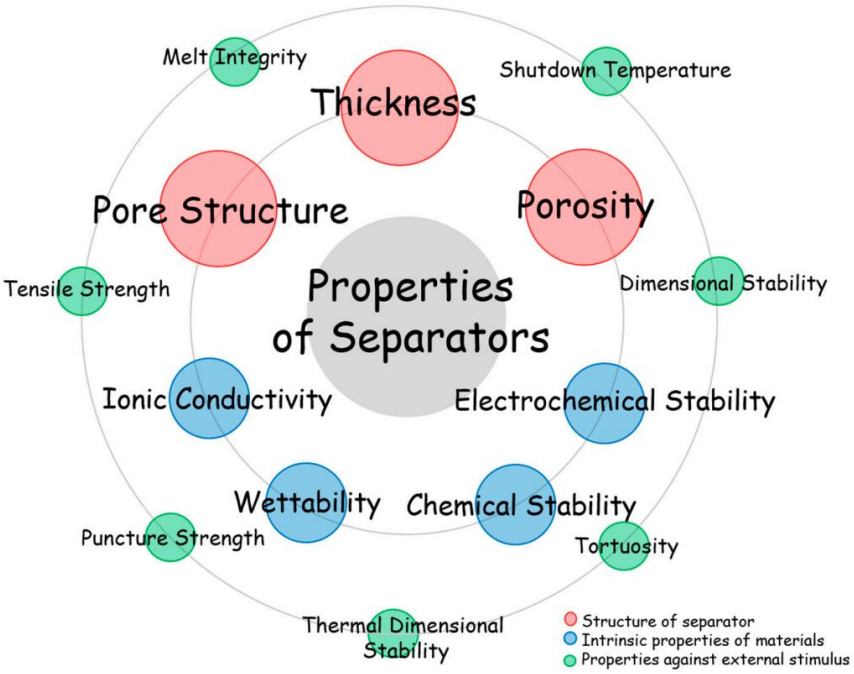

Figure. 2. Illustration of the key properties of separators [4]

Commercial polyolefin separators provide a practical platform to study these couplings because they combine distinct microstructures with different polymer compositions. Table 1 compiles representative specifications for widely used separators, including Celgard 2400, Celgard 2500, Celgard 2325, and Nanoshel polyethylene separator. Even within similar thickness ranges, these materials differ in pore size, porosity, and Gurley value, which together reflect the effective transport resistance set by the pore network. They also differ in mechanical metrics such as tensile strength and puncture strength that influence tolerance to deformation and contact with protruding lithium features. These differences suggest that separator performance cannot be assumed to be universal across cell configurations. In half cells focused on lithium deposition and stripping, transport resistance and wettability can strongly shape lithium ion flux uniformity and interfacial impedance. In full cells operated at high voltage, the same transport factors interact with oxidative stability and species crossover, which can alter cathode side reactions, increase polarization, and shift failure pathways.

Table. 1. Basic properties of the commercial polyolefin separators

Basic Film Properties	Celgard 2400 (PP)	.Celgard 2500 (PP)	Celgard 2325 (PP/PE/PP)	Nanoshel PE
Thickness (μm)	25	25	25	16
Pore Size (μm)	0.043	0.064	0.028	0.060
Gurley (JIS) (Seconds)	620	200	645	350-550
Porosity (%)	41	55	39	38-44
TD Shrinkage @ 105°C / 1 Hour (typical) (%)	0	0	0	⩽ 3
MD Shrinkage @ 105°C / 1 Hour (typical / max) (%)	2.3/5.0	1.1/5.0	3.0/5.0	⩽ 5
TD Tensile Strength (typical / min) (Kg/cm^2)	140/70	130/80	150/80	> 100 MPa
MD Tensile Strength (typical / min) (Kg/cm^2)	1420/700	1170/770	1900/1000	> 90 MPa
Puncture Strength (typical / min) Grams Force (gf)	450/340	325/200	450/380	> 300

Motivated by the conceptual mechanism in Figure 1, the property framework in Figure 2, and the practical parameter differences summarized in Table 1, this work evaluates how separator selection governs electrochemical outcomes across both lithium copper half cells and lithium to NMC full cells under controlled cycling protocols. The objective is to connect separator transport resistance, pore connectivity and other properties to measurable signatures of degradation, including polarization growth, lithium inventory loss, and failure modes such as short circuits, and to determine which separator attributes remain predictive when moving from half cell screening to application relevant full cell conditions.

2. Material/Equipment Sources and Procedures

2.1 Material and Equipment Sources

Commercial NMC811 cathode sheets ($LiNiCoMnO_2$, Ni:Co:Mn = 8:1:1) coated on aluminum foil (single-side coated; 241 mm × 200 mm) were purchased from MTI Corporation (SKU: bcaf-ncm811ss). Lithium metal chips were purchased from MTI Corporation. Commercial polypropylene separators (Celgard 2400, 2500, and 2325) and polyethylene separators (Nanoshel) were used as received. Lithium bis(fluorosulfonyl)imide (LiFSI), 1,2-dimethoxyethane (DME), and 1,1,2,2-tetrafluoroethyl 2,2,3,3-tetrafluoropropyl ether (TTE) were purchased from Gotion.

All hardware components for CR2032-type coin cells were purchased from MTI Corporation, including the anode and cathode cases, stainless-steel spacers (1.0 mm thick), and stainless-steel springs. Copper foil, carbon-coated aluminum foil, a doctor blade, and an electrode coater were also purchased from MTI Corporation. Electrochemical cycling was performed using Neware and Arbin battery test systems.

2.2 Experimental Procedure

The electrolyte was prepared in an Ar-filled glove box by dissolving lithium bis(fluorosulfonyl)imide (LiFSI, Gotion) in a mixed solvent of dimethoxyethane (DME) and 1,1,2,2-tetrafluoroethyl 2,2,3,3-tetrafluoropropyl ether (TTE). The final electrolyte composition

was 1.2 M LiFSI with a molar ratio of LiFSI:DME:TTE = 1:1.2:3. All preparation procedures were carried out under an inert atmosphere to minimize exposure to moisture and oxygen. All the electrochemical tests were performed at room temperature. CR2032 coin cells were assembled in an argon-filled glovebox. Prior to assembly, all components were prepared with fixed dimensions to ensure consistency across cells. Lithium metal chips with a thickness of 250 μm and a diameter of 15.6 mm were used. Copper foil current collectors (9 μm thick) were punched into 19 mm diameter disks for Li|Cu half cells. Commercial NMC811 cathode sheets were punched into 12 mm diameter disks for NMC811|Li full cells. Polymeric separators were punched into 19 mm diameter disks. Separators were dried under vacuum in a drying oven at 60 °C for 24 h prior to use.

Coin-cell hardware, including the anode and cathode cases, stainless-steel spacers (1000 μm thick), and wave springs (1.2 ± 0.05 mm), was dried prior to transfer into the glovebox. Cell assembly followed a consistent stacking order. The cell case was used as the base, and the working electrode disk was placed concentrically in the center. A dried separator was then placed on top to fully cover the electrode surface. Cells were flooded with 100 μL of electrolyte to ensure complete wetting of the separator. The counter electrode was then placed on top, followed by the stainless-steel spacer and wave spring to provide uniform stack pressure. Finally, the cell was sealed using a coin-cell crimping machine.

After crimping, assembled cells were rested in the glovebox prior to testing to promote electrolyte wetting and interfacial equilibration. Li|Cu half cells employed Cu foil as the working electrode and Li metal as the counter electrode. NMC811|Li full cells employed commercial NMC811 cathodes paired with Li metal anodes. All cells were labeled and transferred to the battery test systems for galvanostatic cycling according to the protocols described above.

3. Methods, Results and Discussion

3.1 Methods

Li||Cu coin cells were assembled using lithium metal chips (250 μm thick, 15.6 mm diameter) as

the counter electrode and copper foil (9 μm thick, 19 mm diameter) as the working electrode. A stainless-steel spacer (1000 μm thick) and a wave spring (1.2 ± 0.05 mm) were used. Each separator was evaluated using eight replicate cell. Cells were flooded with 100 μL of electrolyte (M47, 1.2 M LiFSI in DME with TTE). Lithium plating/stripping measurements were performed on a Neware battery tester following an Aurbach-type protocol. The cells were first rested for 2 h, followed by a reservoir-establishment sequence conducted galvanostatically at 0.4 mA cm^{-2}. Repeated plating/stripping cycling was then carried out at 0.4 mA cm^{-2} with an areal capacity of 0.5 mAh cm^{-2} per half-cycle for 10 cycles. Lithium stripping was terminated at 1.0 V. Coulombic efficiency was calculated as the ratio of stripped capacity to plated capacity for each cycle, and the average CE was calculated from cycles 2 to 10. NMC811||Li coin cells were assembled using lithium metal chips (250 μm thick, 15.6 mm diameter) and commercial NMC811 cathodes (12 mm diameter), together with a stainless-steel spacer (1000 μm thick) and a wave spring (1.2 ± 0.05 mm). Each separator was evaluated using five replicate cells. Cells were flooded with 100 μL of electrolyte (M47, 1.2 M LiFSI in DME with TTE). Galvanostatic cycling was performed on an Arbin battery test system between 2.8 and 4.4 V. Two formation cycles were performed at C/10, followed by cycling with C/10 charge and C/3 discharge.

3.2 Results and Discussion

3.2.1 Effect of Separator on Lithium Plating and Stripping

Figure 3 compares the coulombic efficiency of lithium plating and stripping measured with different commercial separators. The results show a clear dependence on separator choice, while all samples remain within a high-efficiency range. Cells assembled with Celgard 2400 and Celgard 2500 consistently exhibit higher coulombic efficiency than those using the Nanoshel polyethylene separator. Among the separators evaluated, Celgard 2400 delivers the highest average coulombic efficiency, whereas the Nanoshel polyethylene separator shows the lowest average value. Celgard 2325 produces an intermediate performance, lower than Celgard 2400 and Celgard 2500 but slightly higher than the Nanoshel polyethylene separator. In addition to the differences in average

values, the distribution of the data indicates measurable cell-to-cell variability, highlighting the need to consider both mean performance and reproducibility when benchmarking separator effects on lithium plating and stripping reversibility.

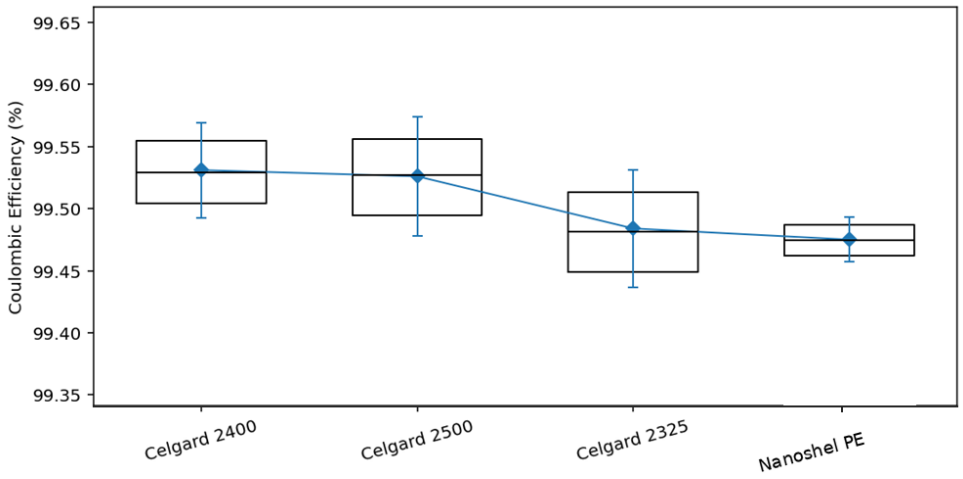

Figure. 3. Coulombic efficiency of lithium plating and stripping measured in Li|Cu half cells using an Aurbach-type protocol with different commercial separators

The separator-dependent trend in lithium plating and stripping coulombic efficiency can be discussed directly from the reported thickness, pore size, porosity, Gurley value, and mechanical strength. Celgard 2400 and Celgard 2500 have the same nominal thickness of 25 μm, and both deliver higher coulombic efficiency than the polyethylene separator under the present Li plating and stripping protocol. Relative to Celgard 2400, Celgard 2500 shows a larger pore size and higher porosity together with a much lower Gurley value, indicating a more permeable pore network and lower effective transport resistance. In contrast, Celgard 2400 has a smaller pore size and a higher Gurley value, implying a tighter pore structure. The fact that Celgard 2400 nevertheless achieves the highest average coulombic efficiency suggests that, within this high-efficiency regime, lithium deposition reversibility is not governed solely by minimizing transport resistance. A moderately smaller pore size and more restrictive pore network may help suppress highly localized ionic pathways and reduce the propensity for nonuniform deposition that produces electrically isolated lithium and additional parasitic reactions, thereby improving the apparent plating and stripping efficiency. Celgard 2325 provides an instructive comparison, as it combines the smallest pore size

with the highest Gurley value and the lowest porosity among the Celgard separators, a set of parameters consistent with the strongest transport limitation. Greater transport limitation can increase polarization and steepen concentration gradients during plating and stripping, which can promote spatially heterogeneous lithium growth even when the nominal pore size is small, offering a plausible explanation for why Celgard 2325 does not outperform Celgard 2400. The polyethylene separator has a nominal thickness of 16 μm, a pore size comparable to Celgard 2500, and intermediate Gurley and porosity ranges, yet it yields the lowest average coulombic efficiency in this dataset. Its lower reported puncture strength relative to Celgard 2400 indicates reduced mechanical robustness, which may allow more pronounced local deformation under stack pressure and evolving interfacial contact during cycling, thereby contributing to less consistent lithium deposition and a lower average efficiency. Overall, these comparisons support a separator effect in which coulombic efficiency reflects a balance between ion-transport characteristics and mechanical integrity, with Celgard 2400 providing the most favorable combination under the conditions studied.

3.2.2 The source of fluctuations

For Table 2, the standard deviation in coulombic efficiency observed for cells employing different separators may be influenced, at least in part, by the limitations of the commercial charge–discharge equipment rather than arising solely from intrinsic electrochemical differences. As reported in the literature, commercial battery testing systems differ in current resolution, voltage resolution, measurement accuracy, and sampling interval. [5] These differences imply that the ability of each instrument to detect small changes in current or voltage is not identical. Even when two systems are nominally described as having 16 bit resolution, their practical accuracy and stability may still vary considerably. A tester with high nominal resolution may nonetheless introduce measurable uncertainty if its current or voltage accuracy is limited. In addition, sampling interval can further affect data quality, since systems with longer intervals may fail to capture rapid transient variations that would be more reliably recorded by instruments with higher acquisition

frequency. Therefore, when the cycle-to-cycle variation in coulombic efficiency is small, part of the observed fluctuation may reasonably be attributed to instrument-dependent factors, including measurement uncertainty, limited accuracy, and differences in data acquisition conditions. In this sense, the standard deviation reported in Table 2 should not be interpreted exclusively as a reflection of separator-induced electrochemical behavior, but rather as the combined result of intrinsic cell response and the technical constraints of the measurement system.

Table. 2. Average Coulombic Efficiency and Standard Deviation of Lithium Plating/Stripping Coulombic Efficiency in Li|Cu Cells for Each Separator Based on Eight Cells

Separator Materials	Average Coulombic Efficiency (%)	Standard Deviation
Celgard 2400 (PP)	99.531	0.0385
Celgard 2500 (PP)	99.526	0.0480
Celgard 2325 (PP/PE/PP)	99.484	0.0472
Nanoshel PE	99.475	0.0180

3.2.3 Effect of separators on Lithium metal full cells

Figure 4 shows the full-cell cycling behavior of NMC811|Li cells assembled with different separators in terms of specific capacity retention and coulombic efficiency. Among the separators evaluated, the Nanoshel polyethylene separator exhibits the most favorable overall performance. The PE-based cell maintains the highest specific capacity over the tested cycle range and shows the most stable capacity trajectory, indicating improved long-term cycling stability relative to the Celgard separators. Consistent with the capacity trend, the coulombic efficiency of the PE-based cell remains close to unity with minimal fluctuation throughout cycling, suggesting more reversible charge–discharge behavior and a lower incidence of parasitic processes that would otherwise accumulate as capacity fade. In contrast, cells using Celgard separators show either lower retained capacity or increasing instability at extended cycles, most prominently for Celgard 2325, which displays an abrupt capacity loss accompanied by pronounced deviations in coulombic efficiency at later cycles. Collectively, these results indicate that, under the high-voltage full-cell environment, the polyethylene separator provides a more robust operating window, supporting both higher deliverable capacity and more stable coulombic efficiency during long-term cycling.

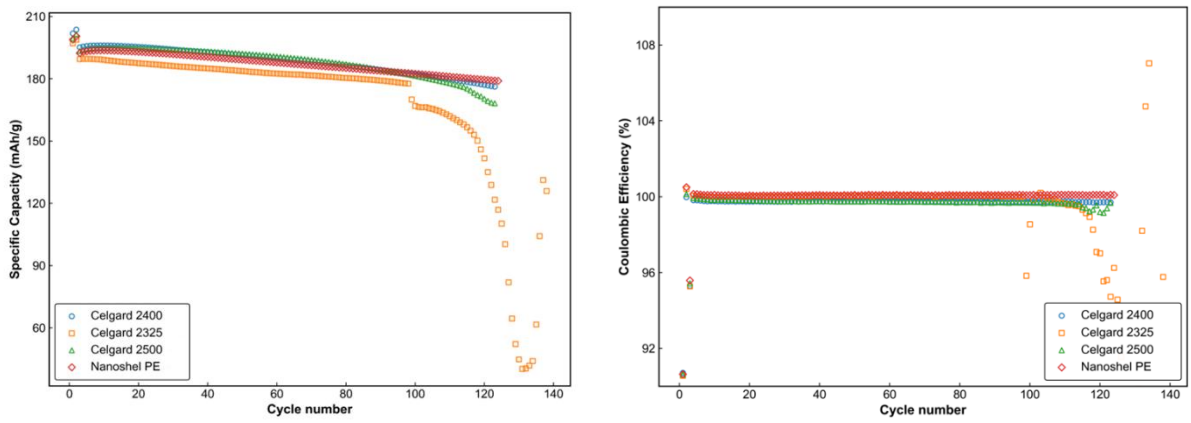

Figure. 4. Cycling performance and long-term cycling stability of NMC811|Li full cells using different commercial separators, including Celgard 2400, Celgard 2325, Celgard 2500 and Nanoshel PE

In the high-voltage NMC811|Li full-cell configuration, the superior capacity retention and more stable coulombic efficiency observed with the Nanoshel polyethylene separator can be interpreted primarily in terms of separator electrochemical stability under oxidative conditions. Prior work on high-voltage Li-ion cells has shown that separator surfaces can participate in interfacial reactions during charging, and that these reactions generate surface deposits derived from electrolyte components. Such deposits increase interfacial and transport impedance, which in turn accelerates polarization growth and amplifies cell-to-cell instability during extended cycling. Within this framework, polyethylene-based separators are generally reported to exhibit higher oxidative stability than polypropylene-based membranes, leading to fewer reaction products on the separator surface and consequently a slower impedance rise at elevated potentials. [6] Translating this mechanism to the present NMC811 full-cell results, the PE separator is expected to better preserve ionic transport pathways and interfacial stability at the cathode-side environment near the upper cut-off voltage, thereby sustaining higher deliverable

capacity and maintaining higher coulombic efficiency over long-term cycling. By contrast, polypropylene-rich separators are more susceptible to high-voltage surface reactions, which can promote deposit formation and progressive transport limitation, consistent with the earlier onset of capacity divergence and the larger efficiency perturbations observed for the less stable separator conditions.

Although Celgard 2325 contains a polyethylene component, its trilayer architecture can still be disadvantaged in NMC811|Li full cells because the electrolyte first encounters polypropylene-rich outer surfaces and a relatively transport-limited pore network. In this dataset, Celgard 2325 has the smallest reported pore size and the highest Gurley value among the commercial separators, indicating a tighter pore structure and a higher effective resistance to gas flow that often correlates with more tortuous ion transport in liquid electrolyte. Under high-voltage cathode operation, electrolyte oxidation and salt or solvent decomposition can generate insoluble or weakly soluble species that deposit on porous interfaces and progressively narrow active pathways, which accelerates impedance growth and polarization during cycling. Prior work has shown that separator surfaces can accumulate such deposits at elevated potentials and that the extent of deposit formation depends on separator chemistry and surface stability, linking separator-side interfacial processes to performance decay in high-voltage cells. [6] For a separator with already restrictive transport characteristics, even modest pore narrowing can disproportionately increase ionic resistance, promote local concentration gradients, and amplify nonuniform current distribution, which is consistent with the abrupt capacity collapse and strong coulombic-efficiency perturbations observed for Celgard 2325 at later cycles. In addition, the polypropylene outer layers are generally harder to wet than polyethylene, so

incomplete or less stable wetting can reduce the effective conducting cross section and further increase local transport limitation. [7] Taken together, these factors provide a plausible explanation for why Celgard 2325 performs worst in NMC811|Li full cells despite containing polyethylene, since its macroscopic behavior is governed not only by polymer composition but also by which polymer is presented at the separator surface and how the overall pore network responds to high-voltage interfacial byproduct accumulation.

4. Conclusions and Future work

4.1 Conclusions

The Li|Cu half-cell measurements of lithium plating and stripping showed consistently high coulombic efficiency for all separators, while still exhibiting a discernible separator dependence. Celgard 2400 produced the highest average coulombic efficiency among the tested membranes, whereas the Nanoshel polyethylene separator exhibited the lowest mean value, with Celgard 2500 and Celgard 2325 showing intermediate performance. This ranking indicates that separator properties can measurably influence lithium deposition and dissolution reversibility even when differences are confined to a narrow, high-efficiency regime. The superior performance of Celgard 2400 in Li plating and stripping is consistent with its separator characteristics, which likely provide a more favorable balance between regulating ion transport and maintaining stable interfacial conditions during cycling. In addition, the small standard deviations observed across replicate cells are within a range where instrument-dependent factors can contribute, because coulombic efficiency is calculated from measured capacities and is highly sensitive when values are close to unity. Using a cycler with higher current and

voltage precision and higher data-acquisition fidelity would reduce measurement-related uncertainty and is expected to decrease the apparent fluctuation.

The NMC811|Li full-cell tests demonstrated that separator ranking can change under high-voltage cycling, highlighting that half-cell reversibility metrics do not fully capture the degradation pathways active in application-relevant full cells. Under the 2.8–4.4 V cycling protocol, the Nanoshel polyethylene separator delivered the most favorable overall behavior, including higher retained capacity, coulombic efficiency that remained closer to unity, and improved long-term cycling stability relative to the Celgard separators. In contrast, Celgard 2325 showed the poorest stability, characterized by an abrupt capacity loss accompanied by pronounced deviations in coulombic efficiency at extended cycles. These outcomes are consistent with the fact that full-cell performance depends not only on baseline separator transport resistance, but also on cathode-side interfacial processes, including oxidative electrolyte decomposition and the accumulation of surface deposits that increase impedance and can restrict effective ion transport. Within this framework, polyethylene-based separators can provide a practical advantage in high-voltage environments by better preserving interfacial stability and sustaining conductive pathways, whereas multilayer PP/PE/PP structures may remain vulnerable if their PP-rich outer surfaces and tighter pore network amplify polarization growth as interfacial byproducts accumulate. Collectively, the paired half-cell and full-cell results support a separator-centered evaluation strategy in which Li|Cu testing serves as a controlled screen for plating and stripping reversibility, while high-voltage full-cell cycling is required to validate separator suitability under cathode-driven degradation conditions.

4.2 Future work

A mechanistic understanding of the separator dependence observed in lithium plating and stripping requires directly correlating separator properties with ion-transport behavior and lithium deposition morphology. To verify the origin of Celgard 2400's superior performance, lithium deposition uniformity will be quantified by top-view and cross-sectional scanning electron microscopy after controlled plating, with emphasis on surface roughness, thickness distribution, and the formation of porous or filamentary lithium features. Separator-limited transport will then be assessed by electrochemical impedance spectroscopy using symmetric-cell configurations, where the incremental resistance per separator layer will be obtained from the linear fit of total resistance versus the number of separators and used to determine effective separator conductivity and the MacMullin number. In parallel, potential short-circuit signatures will be monitored through abrupt voltage or impedance drops to evaluate whether separator mechanical integrity contributes to suppressing lithium protrusion-induced failure. Finally, electrolyte wettability will be compared through contact-angle measurements to quantify differences in wetting behavior that can alter the effective conducting cross-section and local ion-flux distribution. Together, these measurements are expected to establish a quantitative property–performance relationship for Celgard 2400 and provide separator-centered design guidelines for improving lithium plating and stripping reversibility.

The separator ranking observed in the NMC811|Li full cells motivates a more direct interrogation of separator stability under high-voltage conditions using complementary physicochemical diagnostics reported in prior studies. Specifically, the same set of commercial separators will be evaluated before and after high-voltage cycling to determine whether

separator-dependent surface reactions and byproduct accumulation correlate with the divergence in capacity retention and coulombic-efficiency stability. This effort will combine electrochemical signatures with post-mortem characterization, including spectroscopic analyses of separator surfaces and related control measurements designed to isolate cathode-side oxidative effects. Beyond the NMC811|Li configuration, extending the separator comparison to additional lithium battery chemistries will be essential for establishing generalizable selection criteria. The same separators will therefore be benchmarked in representative systems that impose distinct failure modes and interfacial constraints, including lithium–sulfur cells, conventional lithium-ion cells, and anode-free lithium-metal cells. By systematically mapping how separator chemistry and structure interact with electrolyte composition, voltage window, and active-material chemistry across these platforms, the long-term objective is to develop separator-selection guidelines that are explicitly conditioned on battery chemistry and operating environment, rather than relying on a single screening metric or a one-system ranking.

Acknowledgement

I would like to express my sincere gratitude to Professor Jun Liu for welcoming me into the lab and for giving me the opportunity to join the group. I truly cherish this experience, and I am grateful for Professor Liu's support and guidance throughout my master's research. I would also like to thank Dr. Mitchell Kaiser and Peng Zhi for trusting me to participate in their battery research project. When I first started working in the battery field, I had limited experience, and their patience, mentorship, and technical guidance helped me build a solid foundation in electrochemical research. The skills and research mindset I gained through this project have

been essential to my growth and will continue to benefit my future work.

In addition, I would like to extend my sincere thanks to Bella Wu, Anthony Romero, Trung Nguyen, and Minh Duong for their generous help and collaboration during this research. They shared valuable knowledge, offered practical advice, and provided support whenever I encountered challenges. I am grateful for the friendly and encouraging environment in the lab, and I deeply appreciate everyone who contributed to my progress and made this experience meaningful.

References

[1] Cheng, X.-B.; Zhang, R.; Zhao, C.-Z.; Zhang, Q. Toward Safe Lithium Metal Anode in Rechargeable Batteries: A Review. *Chemical Reviews* **2017**, *117*, 10403–10473. DOI: 10.1021/acs.chemrev.7b00115

[2] Arora, P.; Zhang, Z. Battery Separators. *Chemical Reviews* **2004**, *104*, 4419–4462. DOI: 10.1021/cr020738u

[3] Li, C.; Liu, S.; Shi, C.; Liang, G.; Lu, Z.; Fu, R.; Wu, D. Two-dimensional molecular brush-functionalized porous bilayer composite separators toward ultrastable high-current density lithium metal anodes. *Nature Communications* **2019**, *10*, 1363. DOI: 10.1038/s41467-019-09211-z

[4] Jang, J.; Oh, J.; Jeong, H.; Kang, W.; Jo, C. A Review of Functional Separators for Lithium Metal Battery Applications. *Materials* **2020**, *13*, 4625. DOI: 10.3390/ma13204625

[5] Smith, A. J.; Burns, J. C.; Trussler, S.; Dahn, J. R. Precision Measurements of the

Coulombic Efficiency of Lithium-Ion Batteries and of Electrode Materials for Lithium-Ion Batteries. *J. Electrochem. Soc.* **2010**, *157* (2), A196–A202. DOI: 10.1149/1.3268129

[6] X. Chen.; W. Xu.; J. Xiao et al., Effects of cell positive cans and separators on the performance of high-voltage Li-ion batteries, *Journal of Power Sources* 213 (**2012**) 160–168. DOI: 10.1016/j.jpowsour.2012.04.009

[7] Yao, S.; Zhang, T.; Ma, C.; Zhang, C.; Zhang, W.; Shang, J.; Zhang, X.; Liu, H.; Sun, H.; Wang, L.; Xiang, J.; Shen, X. Comparative Study of the Electrochemical Performances of Different Polyolefin Separators in Lithium/Sulfur Batteries. *Mater. Res. Bull.* **2024**, *171*, 112604. DOI: 10.1016/j.materresbull.2023.112604